Research article

JHEP|Reports

Ketohexokinase inhibition improves NASH by reducing fructose-induced steatosis and fibrogenesis

Emma L. Shepherd,[1,†] Raquel Saborano,[1,†] Ellie Northall,[1] Kae Matsuda,[2] Hitomi Ogino,[2] Hiroaki Yashiro,[3] Jason Pickens,[3] Ryan E. Feaver,[4] Banumathi K. Cole,[4] Stephen A. Hoang,[4] Mark J. Lawson,[4] Matthew Olson,[4] Robert A. Figler,[4] John E. Reardon,[4] Nobuhiro Nishigaki,[2] Brian R. Wamhoff,[4] Ulrich L. Günther,[5] Gideon Hirschfield,[1,6] Derek M. Erion,[3] Patricia F. Lalor[1,*]

[1]*Centre for Liver and Gastroenterology Research and National Institute for Health Research (NIHR) Birmingham Biomedical Research Centre, Institute of Immunology and Immunotherapy, University of Birmingham, Birmingham, UK;* [2]*Takeda Pharmaceuticals Cardiovascular and Metabolic Drug Discovery Unit, Kanagawa, Japan;* [3]*Takeda Pharmaceuticals Gastroenterology Drug Discovery Unit, Cambridge, MA, USA;* [4]*HemoShear Therapeutics, Charlottesville, VA, USA;* [5]*Institute of Cancer and Genomic Sciences, University of Birmingham, Birmingham, UK;* [6]*Toronto Centre for Liver Disease, University of Toronto, Toronto General Hospital, Toronto, Canada*

JHEP Reports **2021.** https://doi.org/10.1016/j.jhepr.2020.100217

Background & Aims: Increasing evidence highlights dietary fructose as a major driver of non-alcoholic fatty liver disease (NAFLD) pathogenesis, the majority of which is cleared on first pass through the hepatic circulation by enzymatic phosphorylation to fructose-1-phosphate via the ketohexokinase (KHK) enzyme. Without a current approved therapy, disease management emphasises lifestyle interventions, but few patients adhere to such strategies. New targeted therapies are urgently required.

Methods: We have used a unique combination of human liver specimens, a murine dietary model of NAFLD and human multicellular co-culture systems to understand the hepatocellular consequences of fructose administration. We have also performed a detailed nuclear magnetic resonance-based metabolic tracing of the fate of isotopically labelled fructose upon administration to the human liver.

Results: Expression of KHK isoforms is found in multiple human hepatic cell types, although hepatocyte expression predominates. KHK knockout mice show a reduction in serum transaminase, reduced steatosis and altered fibrogenic response on an Amylin diet. Human co-cultures exposed to fructose exhibit steatosis and activation of lipogenic and fibrogenic gene expression, which were reduced by pharmacological inhibition of KHK activity. Analysis of human livers exposed to ^{13}C-labelled fructose confirmed that steatosis, and associated effects, resulted from the accumulation of lipogenic precursors (such as glycerol) and enhanced glycolytic activity. All of these were dose-dependently reduced by administration of a KHK inhibitor.

Conclusions: We have provided preclinical evidence using human livers to support the use of KHK inhibition to improve steatosis, fibrosis, and inflammation in the context of NAFLD.

Introduction

Non-alcoholic fatty liver disease (NAFLD) a manifestation of the metabolic syndrome[1] is estimated to affect up to a third of individuals in developed countries.[2] The disease spectrum encompasses simple steatosis to non-alcoholic steatohepatitis (NASH) and cirrhosis. Patients with NAFLD have high mortality and are at an increased risk of suffering adverse cardiovascular events.[3] Given the prevalence, limited treatment options, and cost of screening, new treatments are urgently required. Novel therapeutic candidates must manage the complexity of steatosis, systemic metabolic disturbance, inflammation, and fibrosis to be of benefit to patients. Current treatments begin with lifestyle interventions designed to facilitate weight loss,[1] followed by insulin sensitisers and antioxidants, but outcomes are variable.

The increase in incidence of NAFLD has focussed attention upon causative dietary constituents such as fructose.[2,4] Fructose is increasingly included as an additive in processed foods.[5] Global consumption is increasing, with estimates in the USA suggesting average intakes increased from 37 g in the 1970s to 50 g+ in the current diet.[6,7] This could account for 10% of total calories in some populations. Increased consumption of fructose correlates with increased prevalence of obesity,[5] metabolic syndrome, and fatty liver disease,[8] and fructose consumption is a clear risk factor for development of NAFLD.[9]

Fructose metabolism bypasses the requirement for phosphofructokinase and fructose-1,6-bisphosphatase, which are

Keywords: NAFLD; Metabolism; Fructose; Fibrosis; Treatment; NASH.
Received 30 March 2020; received in revised form 30 October 2020; accepted 8 November 2020Available online 20 November 2020

† Equal first authors.

* Corresponding author. Address: Centre for Liver and Gastroenterology Research and National Institute for Health Research (NIHR) Birmingham Biomedical Research Centre, Institute of Immunology and Immunotherapy, University of Birmingham, Birmingham, UK. Tel.: +44 121 4146967.
E-mail address: p.f.lalor@bham.ac.uk (P.F. Lalor).

rate-limiting for glycolysis and gluconeogenesis. Thus, fructose drives hepatic fatty acid synthesis and *de novo* lipogenesis (DNL) via pyruvate and acetyl-CoA formation. Activation of key transcription factors such as SREBP1c[10] and ChREBP enhances DNL through upregulation of fatty acid synthase and acetyl-CoA carboxylase.[11] The majority of circulating fructose is cleared on first pass through the hepatic circulation[12] by the ketohexokinase (KHK) enzyme. Fructose, like glucose, can also be metabolised by hexokinase, although the affinity for fructose is much less,[13] meaning activity of KHK predominates. The two KHK isoforms a and c vary in expression. KHKc has a higher affinity for fructose, and exposure to fructose increases the hepatic expression of both isoforms.[10,13] Thus, in the context of Western diet consumption, conditions favour maximal hepatic exposure to fructose and the potential for unchecked promotion of DNL.

Importantly, little is known about the hepatic response to fructose in subjects with NAFLD[6] with a paucity of mouse and particularly human data describing the physiological consequences of fructokinase inhibition. The evidence above provides a basis to consider inhibition of KHK as a potential therapy in NAFLD. Targeting steatosis and NASH by interference with KHK function should reduce lipogenesis, free fatty acid, and triglyceride (TG) generation.[14] Here, we report unique studies testing whether pharmacological inhibition of KHK alters the outcome of fructose administration.

Materials and methods

Human tissue

Tissue was collected at the Liver and Hepatobiliary Unit, Queen Elizabeth Hospital, Birmingham, UK, with prior informed patient consent and research ethics committee approval (06/Q702/61). Normal tissue was surplus to requirement for transplantation, whereas diseased tissue was collected from explanted cirrhotic livers (primary biliary cholangitis [PBC], alcohol-related cirrhosis [ALD], and NASH). Matched clinical data are summarised in Table 1.

Human primary liver cell cultures

Human explanted liver tissue was used to isolate hepatocytes,[15] hepatic stellate cells (HSCs),[16] activated liver myofibroblasts (aLMFs),[16] hepatic sinusoidal endothelial cells (HSECs),[16] and biliary epithelial cells (BECs)[17] according to our standard protocols.

Co-culture and hemodynamic exposure of hepatocytes and non-parenchymal cells under NAFLD conditions

A shear-based co-culture device (developed by HemoShear Therapeutics[18]) was used as described.[19] For additional information see Supplementary information, Methods. Cells were treated with media alone or media plus indicated concentrations (from 30 nM to 3 μM) of ketohexokinase inhibitor. The KHK inhibitor PF-06835919 used in these studies was prepared as previously described (WO2017115205A1). Media effluent or cells were collected on days 5, 7, and 10 for analysis of lipid (Nile red stain or TG quantitation), gene expression, and immunofluorescent analysis as previously described.[19]

Determination of effects of KHK inhibition on LX-2 cells

LX-2 cells (S. Friedman, Mount Sinai School of Medicine, New York, NY, USA) were seeded in 24-well plates in DMEM +2% bovine serum albumin. At confluency, wells were scratched and media was replaced with fresh media containing DMSO or 10 μM KHKi (*PF-06835919*), ± transforming growth factor beta 1

Table 1. Demographic information for the transplant tissue donors used in this investigation.

Aetiology	Age (years)	BMI (kg/m^2)	IGF/diabetes (Y/N)	AST (IU/L)	ALT (IU/L)	Platelets (10^9/L)	Albumin (g/L)	FIB4	APRI	Mean KHK
NASH	51	–	Yes	37	24	87	35	2.3129	0.69	2.972
NASH	62	–	Yes	57	36	120	26	2.4636	0.75	0.6356
NASH	75	–	Yes	–	65	133	32	–	1.22	0.7882
NASH	48	43.86	Yes	16	27	204	45	1.5882	0.33	3.14
NASH	59	34.81	No	–	787	58	26	–	33.92	1.325
NASH	55	22	Yes	–	254	70	27	–	9.07	1.225
NASH	59	34.42	No	–	818	64	28	–	31.95	2.569
NASH	68	24.74	Yes	–	1491	122	33	–	30.55	2.318
NASH	63	34.65	Yes	9	15	167	32	1.8862	0.22	0.7227
NASH	68	28.03	Yes	–	541	86	20	–	15.73	2.381
NASH PBC	72	24.92	No	–	1233	112	30	–	27.52	1.382
ALD	58	23.01	No	50	–	84	38	–	1.49	0.1988
ALD	60	34.03	No	16	–	100	45	–	0.4	0.2212
ALD	59	23.27	No	28	–	96	40	–	0.73	0.243
ALD	52	28.35	No	33	–	142	48	–	0.58	0.1922
PSC	61	–	No	66	24	57	26	–	2.89	1.335
PSC	66	24.72	No	–	48	132	36	–	–	1.626
PSC	37	21.73	No	–	1627	199	31	–	–	3.879
PSC	51	29.81	Yes	–	857	126	20	–	–	1.038
PSC	22	20.72	No	–	1595	402	24	–	–	1.927
PBC	54	23.52	No	–	105	78	35	–	–	1.194
PBC	46	–	No	–	1331	92	19	–	–	0.539
NASH PBC	72	24.92	No	–	1233	112	30	–	–	1.511
PBC	71	26.47	No	64	62	95	21	–	0.68	2.563

All details are anonymised data that were available to the researchers from patients where samples were collected at the time of transplant. Matching tissue from each patient was collected for use in experimental analyses. The dash denotes no clinical data available for the indicated variable. Diagnosis at time of transplant (aetiology) and for each tissue sample total *KHK* mRNA expression in whole liver is given (determined by qPCR, see Materials and methods section). Data represent individual expression values compared with the *SRSF4* housekeeping gene. Units for other values are given in the column headings.
ALD, alcohol-related cirrhosis; ALT, alanine transaminase; APRI, AST to Platelet Ratio Index; AST, aspartate transaminase; FIB4, fibrosis-4; IGF, insulin-like growth factor; KHK, ketohexokinase; NASH, non-alcoholic steatohepatitis; PBC, primary biliary cholangitis; PSC, primary sclerosing cholangitis.

(TGFb1) (10 ng/ml) or platelet-derived growth factor-BB (PDGF-BB, 100 ng/ml, Miltenyi Biotec, Woking, UK). Real-time images were captured over a 24-h period in a 5% CO_2 environment at 37°C using a Cell-IQ system (CM Technologies, Oy, Finland) running Imagen software version 2.8.12.0 and analyser version 3.3.0. The percentage closure was determined as previously described.[16]

qPCR

For gene expression analysis, total RNA was prepared from murine and human liver specimens, LX-2 cells, or cells isolated from the HemoShear culture system. Information is supplied in the Supplementary information, Methods.

Western blotting

Human liver tissue prepared and separated on a 10% SDS polyacrylamide gel using standard protocols. Membranes were immunoblotted primary antibodies: KHK, KHKA, KHKC (Signalway Antibody, MA, USA) or β-actin followed by horseradish peroxidase-conjugated secondary antibody diluted in PBS/5% milk/0.1% Tween 20. Detection of the bound antibody was performed using enhanced chemiluminescence Western blotting substrate (ThermoFisher Scientific, Loughborough, UK), and ImageJ software version 1.70_75.

Murine model of NAFLD

Nine-week-old wild-type (WT) and KHK-deficient (Ketohexokinase A and C knockout [KHK-A/C KO], Takeda) litter-mate male C57/BL6 mice were fed high trans-fat/fructose and cholesterol diet (Amylin[20]) or control diet (CE2, CLA Japan: http://www.clea-japan.com/en/diets/diet_a/a_03.html) for up to 29 weeks *ad libitum* (dietary constituents are shown in the Supplementary information, Methods). The diet has been reformulated recently to replace the trans-fat content with palm oil[21] with no significant phenotypic consequence. Blood and tissue samples were collected at 37 and 38 weeks, respectively. Plasma transaminase content was assessed using a 7180 Clinical Analyzer (Hitachi High-Technologies, Tokyo, Japan), and TIMP-1 concentration by ELISA (Mouse TIMP-1 Quantikine ELISA kit, R&D systems, Abingdon, UK). Frozen liver tissue was used for assessment of total TG (E-test Wako; FUJIFILM Wako Pure Chemical Corporation) and collagen concentration (Total Collagen Assay Kit, QuickZyme Biosciences, Leiden, The Netherlands). Urine was used to determine glucose and creatinine concentration using a 7180 Clinical Analyzer. Urinary fructose concentration was detected using EnzyChrom™ Fructose assay kit (Biochain, San Fransisco, USA). All animal experiments were designed and reported under best practice guidelines from ARRIVE and approved by the Institutional Animal Care and Use Committee of Shonan Research Center, Takeda Pharmaceutical Company Limited.

Immunohistochemical and chromogenic staining of human liver tissue

Sections (7 μm thick) of formalin-fixed or snap frozen human or murine liver tissue were stained with H&E or Sirius Red[16] according to standard protocols. For analysis of transporter expression fixed tissue sections were stained using standard indirect immunohistochemical methods as described previously.[16]

Assessment of human liver metabolism by nuclear magnetic resonance

Large superficial vessels in the exposed cut face of freshly cut wedges from donor or human liver specimens from patients with cirrhosis were cannulated to permit media perfusion. Samples were flushed with glucose-free DMEM (Thermofisher) and paired liver samples were then perfused with media alone or KHK inhibitor (10 μM, in glucose-free DMEM containing unlabelled fructose [Sigma, Gillingham, UK]) for 30 min. Subsequently, the wedges were perfused with glucose-free DMEM containing $^{13}C_6$-labelled fructose (20 mM, Cortec Net SA, Paris, France) for up to 3 h. Tissue samples were collected at intervals from 30 min to 3 h and snap frozen or formalin fixed.

Human liver tissue sample extraction, data acquisition, and processing

Tissue samples from perfused livers (100 mg) were added to gentleMACs M-Tubes in cold methanol (8 μl/mg) and purified water (2 μl/mg). Tissue was homogenised (gentleMACs, Miltenyi, UK) and polar metabolites were extracted as described previously.[22] Samples were kept at 4°C before nuclear magnetic resonance (NMR) imaging. All spectra were acquired at 300 K on a Bruker 600 MHz spectrometer with a TCI 1.7 mm z-PFG cryogenic probe using a cooled Bruker SampleJet autosampler as previously described.[22] One-dimensional ^{1}H-NMR spectra were processed using the NMRlab and Metabolab programmes within Matlab, version R2016b (MathWorks, MA, USA). Two-dimensional heteronuclear single quantum coherence (HSQC) spectra processing was initially performed using NMRPipe[23] with the Hyberts extension for processing non-uniformity sampling spectra[24] and subsequent analysis was performed using NMRLab in MATLAB_R2016b (The Mathworks). Cosine-squared window functions were applied to both dimensions and spectra were phased manually. Calibration was carried out manually using L-lactic acid as a reference peak (δ 1.31/22.9 ppm) and scaling was performed using TSA-scaling factors from 1D NOESY (Nuclear Overhauser Effect Spectroscopy) associated spectra. Peak identification used MetaboLab[25] with reference to HMDB (Human Metabolome Database : https://hmdb.ca).

Statistical analysis

Unless otherwise stated, *p* values were calculated using the Student *t* test with 2-way analysis of variance. Murine data were also analysed using 2-way ANOVA with the Tukey post-test to determine effects between groups. Data represent mean values with error bars indicating SEM. Individual symbols indicate a single animal within the group. For transplant patients for whom we had demographic information and explanted liver tissue, we performed Pearson correlation analysis. Here we compared the hepatic KHK mRNA level with standard haematological and biochemical biomarkers.

Results

Mice deficient in KHK show reduced injury and fibrogenesis

WT and KHK A/C-KO mice were fed normal chow or high-trans fat/fructose Amylin diet for 29 weeks. WT mice showed a significant increase in alanine transaminase (AST) and alanine transaminase (ALT) concentrations when exposed to a high-fat diet (Fig. 1A and B). ALT levels were markedly reduced in KO mice on a high-fat diet compared with WT (Fig. 1A). Mice on the Amylin diet also showed development of steatosis as evidenced

by increased hepatic TG content (Fig. 1C, Fig. S1). This was accompanied by increased cholesterol levels, and a modest decrease in circulating TG content (Fig. S1B) as previously reported.[26] Early liver fibrosis was demonstrated by a significant increase in plasma TIMP-1 concentration, total hepatic collagen content, and histological fibrosis area (Fig. 1E and F, Fig. S1A). There was increased transcription of Collagen1a and TIMP-1 in response to diet, with significantly less induction in KHK-KO animals (Fig. 1G). Figure S1C shows that KHK A/C-deficient animals show a significant increase in urinary fructose on the Amylin diet. Thus, deficiency in KHK protects against features of NASH in this murine model.

Inhibition of KHK in human hepatic culture models reduces steatosis and profibrotic responses

Human hepatocellular expression of *KHKa* and *c* was confirmed by qPCR analysis (Fig. S2). Overall transcription of KHK mRNA was similar between normal and fibrotic livers (Fig. S2A). Preliminary correlation analysis of KHK expression and clinical parameters (Figs. S2B and S3 revealed no correlation between hepatic KHK mRNA and biochemical or haematological parameters). We also specifically stratified KHK expression in patients with NASH in the cirrhotic *vs.* fibrotic categories (based on the AST to Platelet Ratio Index [APRI], Fig. S3B) and again there was no correlation.

Expression of KHK was detected in primary human hepatocytes, with modest expression in other epithelial and fibroblast populations (Fig. S2A). This was supported by immunohistochemical staining with a pan KHK antibody (Fig. S2C). Staining was uniformly distributed across the lobule, but macrovesicular steatosis in donor samples led to a concentration of staining at the periphery of steatotic hepatocytes. Expression was concentrated in hepatocytes within regenerative nodules from cirrhotic NASH samples, but intensity of expression was similar between normal and fatty donor liver specimens. We interrogated an open access RNAseq database[27] to assess whether similar patterns of gene expression were evident in hepatic mesenchymal and epithelial populations from normal and cirrhotic livers. Figure S4 confirms that KHK was widely expressed in epithelial and mesenchymal cells in this study, with increased median gene expression in hepatocytes in an uninjured context. In contrast, myofibroblast expression appeared similar in both conditions.

Some studies[13] report that KHKc is the major hepatic transporter under basal conditions. Western blotting showed a reduction in total expression of KHK in cirrhotic liver (ALD and NASH). KHKc was the most abundantly expressed isoform (Fig. S2D). We also confirmed that the major fructose transporters were expressed in the context of human liver disease (Fig. S5). Both GLUT2 and GLUT5 mRNA were present in normal

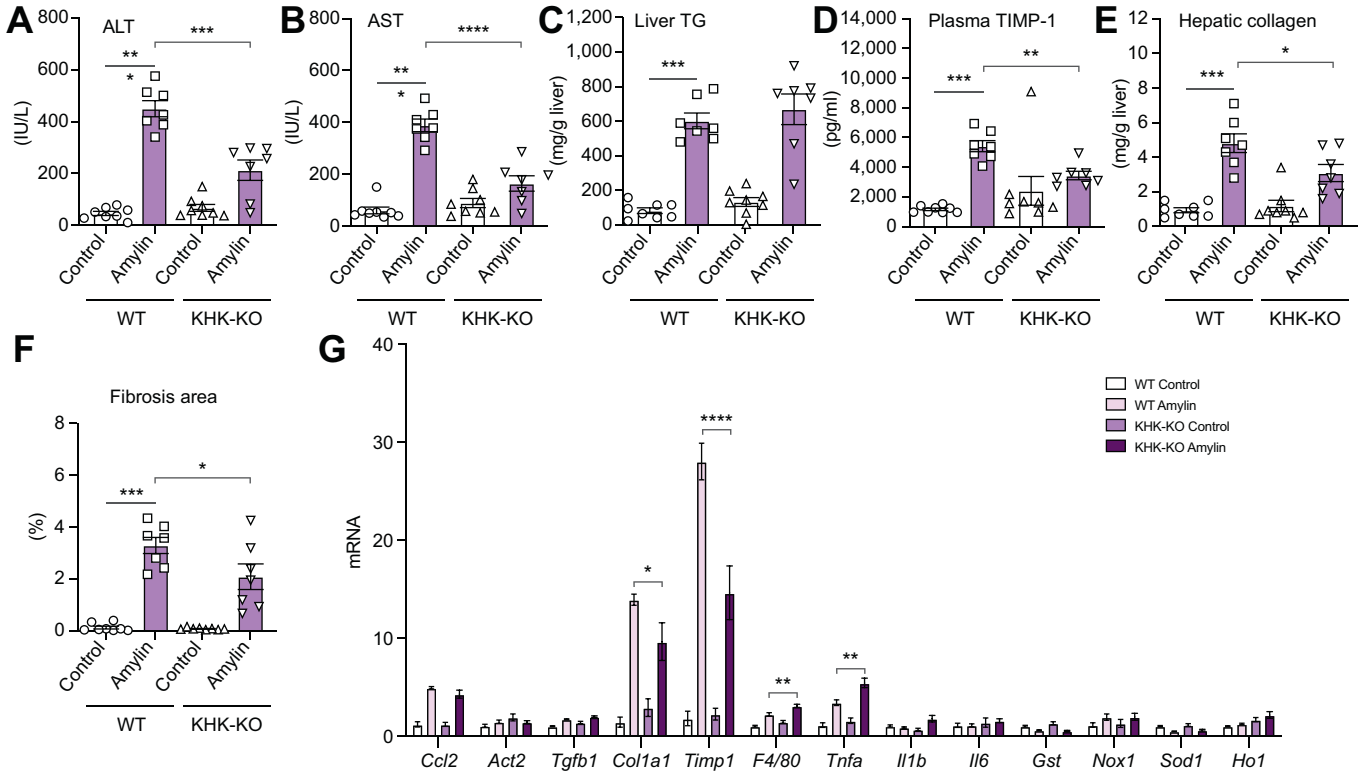

Fig. 1. KHK-deficient mice are protected from the effects of a Western diet. (A–F) WT or KHK-KO mice fed Amylin diet or calorifically matched controls for 29 weeks. Values from 7–8 mice per group are shown with mean and SEM for each cohort. Unpaired *t* tests where **p* <0.05, ***p* <0.001, and ****p* <0.0001, *****p* <0.00001. Two- way ANOVA with Tukey post test for ALT and total fibrosis area for WT and KHK-KO $p = 0.002$ and $p = 0.0299$, respectively. (G) qPCR data are mean ± SEM n = 7–8 mice per group. One-way ANOVA with Tukey post test for WT and KHK-KO mice on the high-fat diet ($p = 0.002$, $p = 0.0001$, $p = 0.0016$, and $p = 0.0014$ respectively). ALT, alanine transaminase; AST, aspartate transaminase; KHK, ketohexokinase; KO, knockout; TG, triglyceride; TIMP-1, Tissue Inhibitor of Matrix metalloproteinase-1; WT, wild-type.

and NASH livers, with modest reduction in simple steatosis. Immunohistochemical assessment of GLUT2 protein confirmed localisation to the sinusoidal face of hepatocytes in normal livers with redistribution to a more cytoplasmic localisation in NASH (Fig. S5).

We utilised a human liver cell culture model[18] where hepatocytes and non-parenchymal cells (NPCs) are co-cultured for 10 days under shear stress and can be treated to recreate either simple steatosis or more advanced NASH pathophysiology. TG accumulation within hepatocytes increased in the presence of glucose and fructose (Fig. 2A and B). Administration of increasing doses of KHK inhibitor to cells treated with both fructose and glucose resulted in dose-dependent inhibition of lipid accumulation (Fig. 2). Both total lipid and specific TG species were increased in cultured cells exposed to glucose and fructose. We also observed a change in hepatocyte lipogenic (*ACLY*, *DGAT-2*, *FASN*, and *SREBP-1*) and fibrogenic (*Col1A1* and *Col4A1*) gene expression in NPCs (Fig. 2C). Inhibition of KHK in the presence of glucose and fructose led to a return of lipogenic gene expression to baseline levels (*FASN*, *ACLY*, and *DGAT-2*, Fig. 3). This was accompanied by a tendency to increase cytoprotective gene expression (HO-1, NQO-1, TXNRD1, and Nrf-2).

We also performed experiments using cultured fibroblast cells (LX-2) to assess whether KHK inhibition can have a direct effect on hepatic fibrosis. Figure 4 shows that administration of KHK inhibitor to LX-2 cells did not significantly alter their phenotypic appearance, viability (not shown), or ability to repair a scratch wound (inset images Fig. 3A). However, we noted a significant reduction in the ability of activated (PDGF exposed) cells to close a wound following treatment with KHK inhibitor. This was accompanied by a significantly reduced profibrogenic gene expression profile. Hence, Col1A1, aSMA, CTGF, PDGFRB,

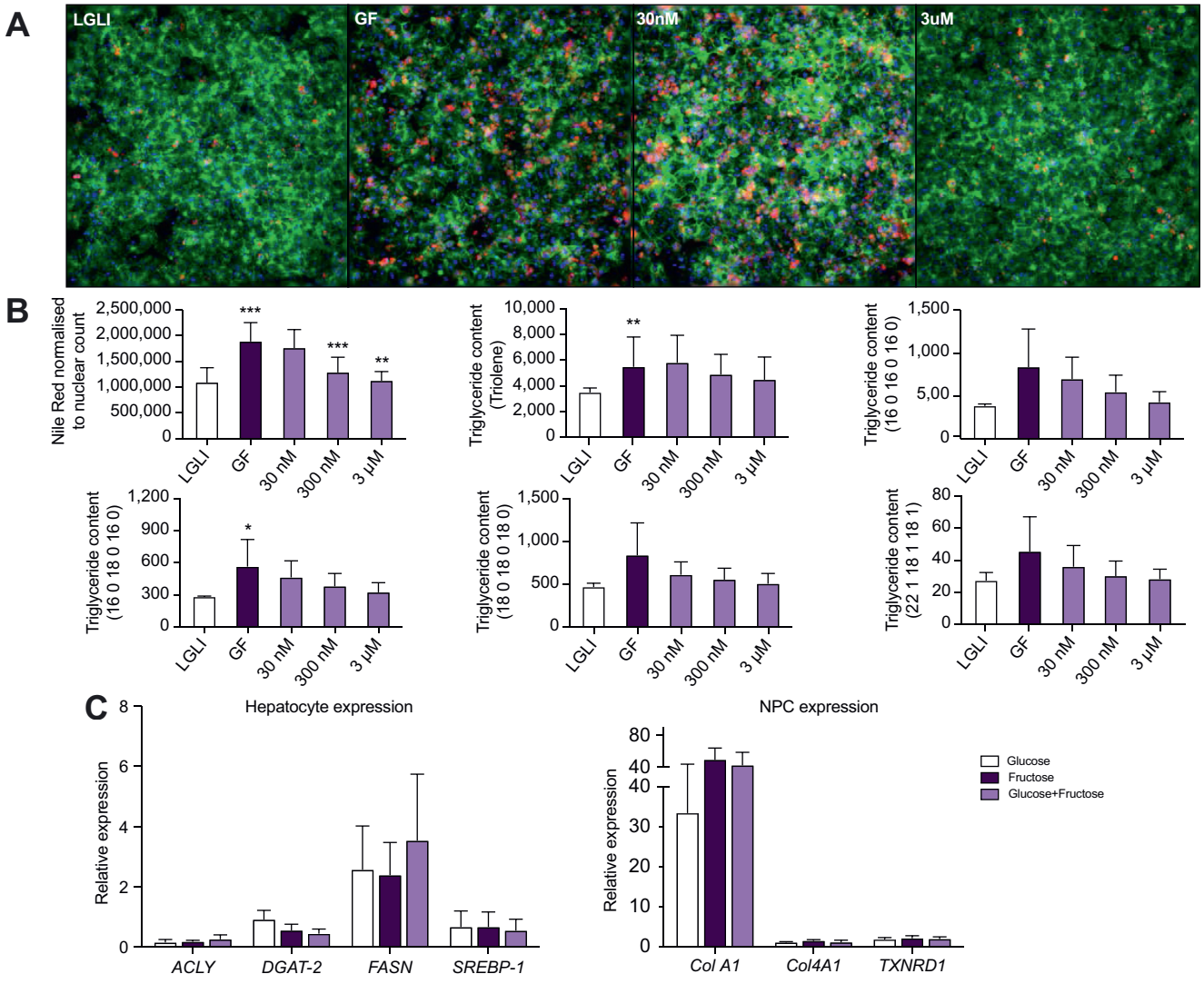

Fig. 2. Fructose administration to human co-cultures results in triglyceride accumulation which is dose-dependently inhibited by KHK inhibition. (A) Cells in low glucose and insulin (5.6 mM and 0.69 nM respectively, LGLI), or glucose/fructose (12.5 mM GF) ± 30 nM to 3 μM KHK inhibitor (PF-06835919). Nuclei (blue), hepatocytes (anti-E-Cadherin, green) Nile red (lipid). (B) Left panel, lipid quantification mean ± SEM, n = 5. Unpaired *t* tests LGLI *vs.* GF $^{**}p$ <0.01 and $^{***}p$ <0.001, KHK inhibitor, $^{**}p$ <0.01, $^{***}p$ <0.001 *vs.* GF. Remaining panels, triglyceride content by mass spectrometry ($^{*}p$ <0.05, **p <0.01 *vs.* LGLI). (C) qPCR for cells in 25 mM glucose/fructose (25 mM) alone or 12.5 mM each. Expression *vs. NONO*/*PGK1*/*RPS11* housekeeping genes mean ± SEM of N = 5. KHK, ketohexokinase; GF, glucose/fructose; LGLI, low glucose and insulin.

and LOX expression reduced in TGFB-stimulated cells exposed to KHK inhibitor.

Human livers exhibit a rapid lipogenic response after fructose administration, which is modified by administration of KHK inhibitor

We used a perfusion system with viable human liver tissue wedges to confirm the mechanism by which KHK inhibition alters hepatic lipid accumulation (Figs. 5 and 6 and Fig. S6). Freshly harvested normal human liver tissue wedges were perfused with media containing 20 mM $^{13}C_6$-labelled fructose in the presence or absence of 10 μM KHK inhibitor, and tissue samples were collected 30 min to 3 h later. Tissue integrity was confirmed at the start and end of the perfusion period by H&E staining (Fig. 5), and frozen tissue samples were processed for NMR metabolomic analysis. Comparison of the ^{1}H-^{13}C-HSQC spectra from representative control (blue) and KHK inhibited (red) liver samples after increasing perfusion time confirmed that labelled fructose was taken up by the control and inhibitor-treated livers at a similar rate and accumulated over time. Gradual conversion of fructose to glycerol and glycerate was observed in control livers, as was conversion to labelled sorbitol (Fig. 5). Although labelled sorbitol appeared in the KHK inhibited samples, there was a distinct lack of labelled glycerol and glycerate. Quantification of this response is shown in Fig. 6. This confirms that a single administration of KHK inhibitor reduced human hepatic accumulation of labelled lipogenic fructose derivatives. Glycolysis was also altered, as there was little accumulation of lactate (or alanine) after treatment with KHK inhibitor. As labelled fructose was no longer converted to these metabolites in the KHK-inhibited livers, there was a corresponding increase in labelled sorbitol (Fig. 6). We performed a similar analysis of explanted NASH tissue (Fig. S6) and the results were similar, except for a reduced accumulation of labelled carbon in glucose molecules and slower accumulation of labelled fructose in tissue. Thus, we show for the first time in normal and cirrhotic human liver tissue, that fructose uptake results in a rapid conversion to lipogenic precursor molecules. Inhibition of ketohexokinase enzyme activity halts this conversion, reducing TG accumulation, and cellular stress and causes a consequential reduction in fibrogenesis.

Discussion

Increasing evidence highlights fructose as a driver of NAFLD pathogenesis.[5,6,9,28] Acute studies in humans confirm that steatosis is increased after fructose supplementation.[29] Fructose feeding in mice has also been shown to increase hepatic steatosis.[13] KHK-deficient mice are protected from fatty liver disease, with modest changes in fibrogenesis and reduced transaminase level[30] linked to a reduction in hepatic necroinflammatory activity.[13] Importantly, the mechanism by which fructose consumption leads to hepatic steatosis is suggested to be

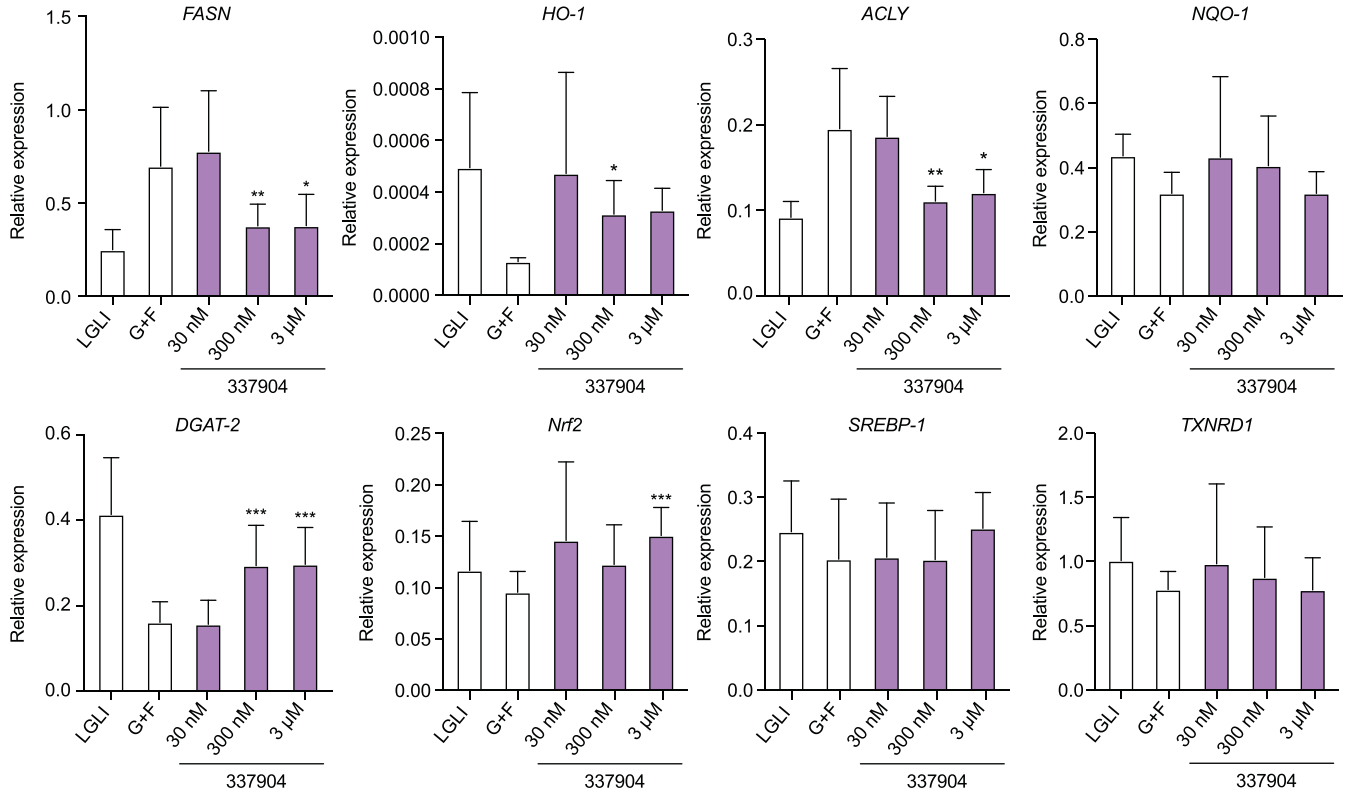

Fig. 3. KHK inhibition reduces lipogenic gene expression while increasing cytoprotective genes in co-cultured human hepatocytes. Taqman PCR assessment in co-cultured hepatocytes in low glucose and insulin (5.6 mM and 0.69 nM LGLI), or glucose/fructose (12.5 mM GF) ± 30 nM to 3 μM KHK inhibitor (PF-06835919) expression *vs. NONO*/*PGK1*/*RPS11* housekeeping genes is mean ± SEM, n = 5 replicate experiments. Where indicated, there was a significant change in gene expression after inhibitor treatment *vs.* GF-treated cells (unpaired *t* tests $^{*}p$ <0.05, $^{**}p$ <0.001, and $^{***}p$ <0.0001). KHK, ketohexokinase; KHKi, KHK inhibited.

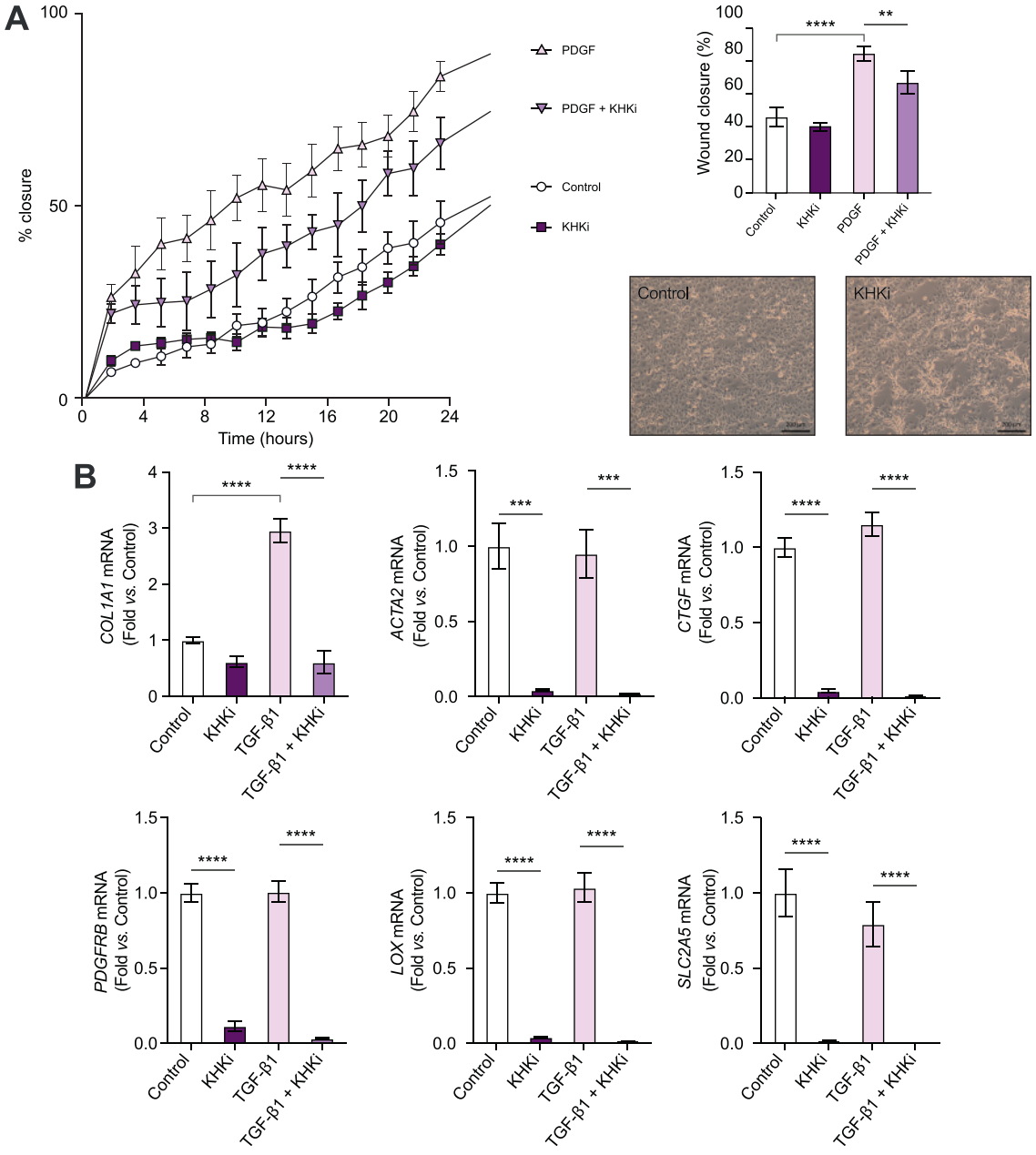

Fig. 4. KHK inhibition reduces fibrogenic gene expression in cultured LX-2 cells. (A) LX-2 cells serum starved (0.2% BSA) for 24 h before the scratch wound ± PDGF-BB and 10 μM KHKi (PF-06835919). Control cells ±100 ng/ml PDGF-BB alone. Data mean ± SEM % closure (left) and at 24 h (right). Images of unscratched wells at 24 h. Unpaired *t* tests $^{**}p$ <0.01 and $^{****}p$ <0.0001. (B) PCR gene expression in LX-2 ± TGFb1 (10 ng/ml) or KHKi (10 μM) for 24 h. Data mean ± SEM fold change in expression *vs.* control untreated cells. Significant change in gene expression (unpaired *t* tests $^{***}p$ <0.0001 and $^{****}p$ <0.00001). BSA, bovine serum albumin; KHK, ketohexokinase; KHKi, KHK inhibited; PDGF, platelet-derived growth factor; TGFb, transforming growth factor beta.

independent of total energy intake.[13,28] Rather, presence of abundant fuel for glycolysis and enhanced acetyl-CoA production promote DNL with accumulation of intermediates of glycolysis providing fuel for glycerol-3 phosphatase and TG synthesis.[31] However, the cellular consequences of administration of fructose on a background of liver disease have yet to be fully characterised, particularly in a human setting. It is also important to acknowledge that there is considerable inter-individual difference between effects of fructose administration in humans, and acute *vs.* chronic dietary administration may have different outcomes.[32]

We have demonstrated that ketohexokinase is abundantly expressed in the cytoplasm of hepatocytes. Onset of metabolic liver disease in the form of steatosis or more significant NASH was not associated with changes in RNA expression, but total protein expression was reduced, probably reflecting the decreased proportion of hepatocytes in fibrotic livers. We also noted a modest increase in expression of the major fructose

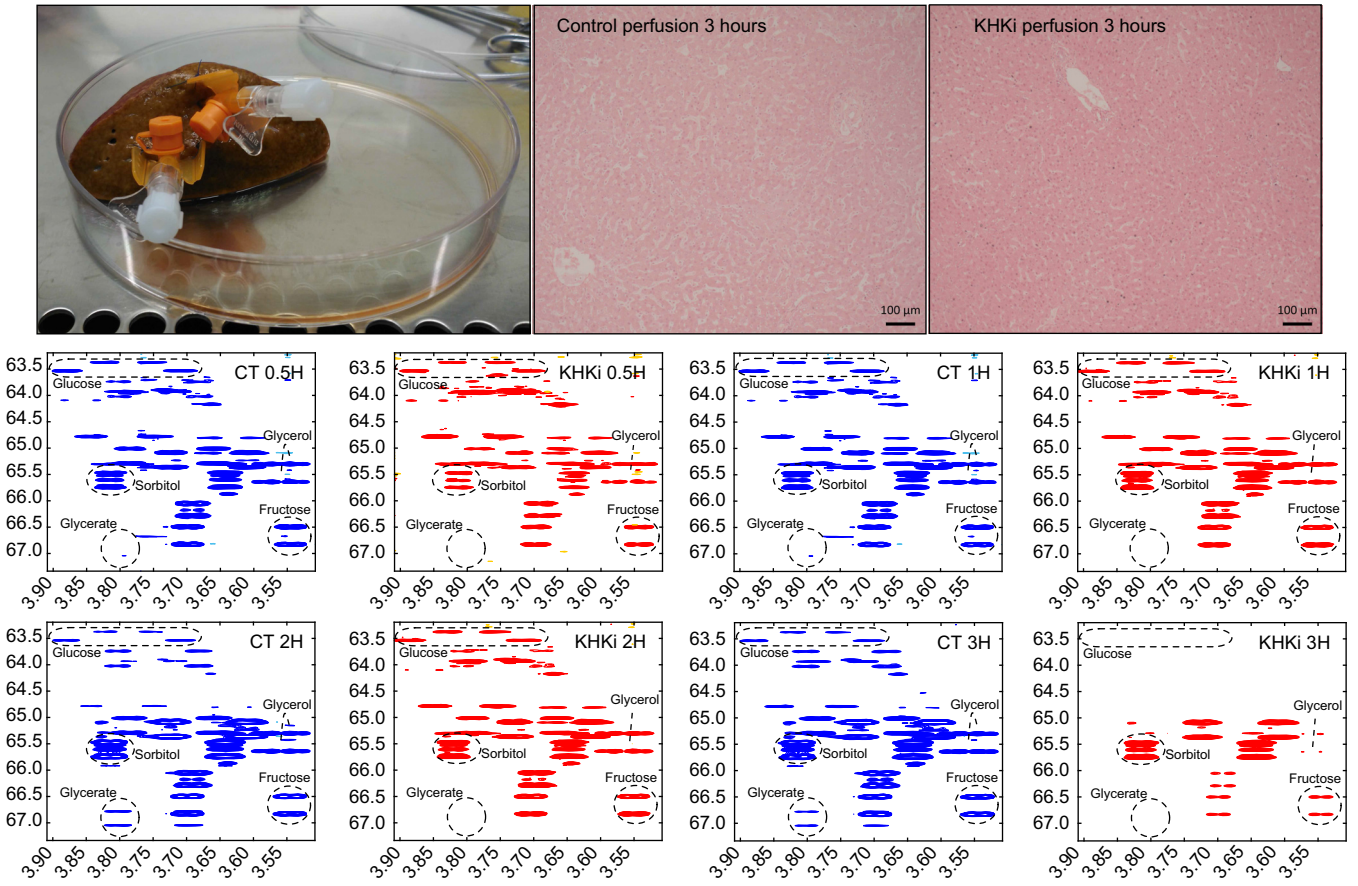

Fig. 5. NMR analysis of perfused human livers exposed to stable isotope-labelled fructose confirms KHK inhibition reduces lipogenesis and glycolysis. Superficial vessels in paired wedges were cannulated (image) to permit delivery of ^{13}C-labelled fructose. Livers maintained at 20°C for up to 3 h with continuous media perfusion, with tissue samples collected at indicated times. Representative H&E stained samples at 3-hour time point (top centre/right images). Graphs represent ^{1}H-^{13}C-HSQC spectra from matched controls (CT: blue) and KHK inhibited (KHKi red) donor liver samples exposed to labelled fructose for indicated periods (30 min to 3 h). Peak assignments are indicated by hashed circles. CT, computed tomography; HSQC, heteronuclear single quantum coherence; KHK, ketohexokinase; KHKi, KHK inhibited; NMR, nuclear magnetic resonance.

transporter GLUT-5 in NASH accompanied by redistribution of GLUT-2 to hepatocyte cytoplasm. Hyperinsulinaemia has been shown to drive enterocyte GLUT-2 redistribution,[33] and similarly fructose increases intestinal GLUT-5 expression.[34] Fructose also drives the differentiation of 3T3L1 adipocytes and increases their expression of GLUT-5.[35] Thus it is likely that in a NASH context, increased dietary fructose increases intestinal uptake[36] and delivery to the liver via the portal vein where liver epithelial populations transport and metabolise the fructose.

We demonstrate that steatosis and serum transaminase elevation are evident in mice fed a high-fat diet supplemented with fructose. KHK-deficiency was protective, leading to a marked increase in urinary fructose excretion as expected.[13] Hepatic steatosis as a result of fructose overload occurs because unregulated glycolysis and gluconeogenesis drive fatty acid synthesis and DNL. Elevated levels of uric acid and increased transaminases correlate with increased fructose uptake,[37] metabolic abnormality, and development of cirrhosis. Importantly, increased uric acid levels are associated with cardiovascular risk in patients with diabetes,[38] thus could contribute to cardiovascular mortality in patients with NASH.[3] Uric acid also causes NFκB activation and liver inflammation,[39] with increased uric acid production and KHK activation/upregulation further exacerbating lipogenic effects in cultured hepatocyte cell lines.[40] Fructose-dependent dysbiosis may also contribute to the pathogenesis of NASH as changes in gut microbiota species are noted in patients with NAFLD related to fructose consumption.[41] This causes changes in gut permeability, increasing hepatic endotoxin exposure[42] and also activates hepatic lipogenesis as a consequence of uric acid metabolism and oxidative stress.[43]

Although the consequences of fructose exposure on a hepatocellular level are well characterised, detailed mechanistic studies defining the metabolic pathways in humans or human cells are rare. It is also notable that use of a global murine KO model cannot discriminate hepatic and extrahepatic effects on the kidney[44] and intestine.[45] We have used a culture system incorporating both hepatocytes and NPCs to dissect the consequences of fructose administration in human NAFLD. Addition of fructose primed TG accumulation and upregulation of lipogenic genes, which was inhibited in the presence of KHK inhibitor. This is in agreement with our animal study where the Amylin diet caused increased hepatic TG accumulation accompanied by reduced TG export. We also observed a reduction in hepatoprotective[46,47] gene expression following fructose administration, and this too could be reversed by KHK inhibition.

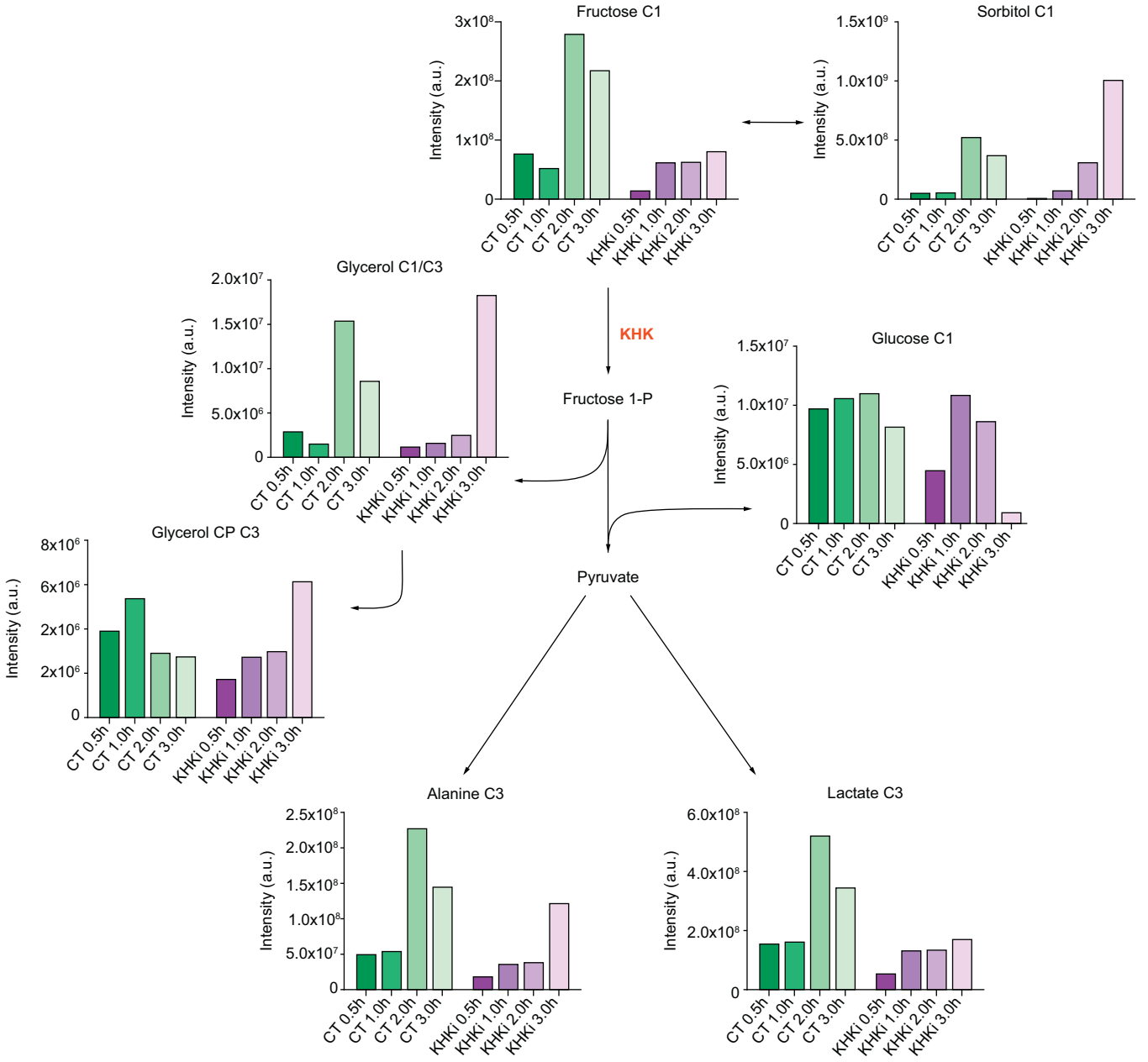

Fig. 6. KHK inhibition reduces lipogenesis and glycolysis in perfused human liver wedges exposed to stable isotope-labelled fructose. Diagrammatic representation of the major fructose metabolism pathway overlaid with ^{1}H-^{13}C-HSQC spectrum integrated peak intensities for indicated metabolites in control (CT: green) or KHK-treated (KHKi: purple) livers over the experimental time course (30 min to 3 h). CT, computed tomography; HSQC, heteronuclear single quantum coherence; KHK, ketohexokinase; KHKi, KHK inhibited.

Previous studies have linked administration of fructose containing diet to humans[48] and exposure of cell lines to fructose *in vitro*[49] with production of chemokines such as CCL2. Much of the profibrotic effect of chemokines such as CCL2 and the CXCR3 ligands relates to their ability to modify hepatic immune cell recruitment and function to promote activation of stellate cells. However, CXCL10 has also been shown to directly mediate stellate cell chemotaxis and RAS-dependent activation.[50] This could explain the early fibrogenesis evident in our mice fed the Amylin diet (Fig. S1A), and the induction of profibrotic genes such as Col1A1 within fructose-exposed NPCs in our co-culture system. Although KHK inhibition may have a predominant effect on parenchymal cells, thereby reducing their production of proinflammatory and profibrotic mediators, it is possible that fructose metabolism can directly promote fibrogenesis through effects on hepatic myofibroblast populations. We showed that both human stellate cells and fibroblasts expressed KHK mRNA, and previous evidence suggests that fructose 1–6 biphosphate can modify cell phenotype to reverse stellate cell activation.[51] This is in agreement with our evidence that interference with fructose metabolite generation through inhibition of hexokinase reduces profibrogenic gene expression in LX2 cells. This suggests that

pharmacological inhibition of KHK has the potential to modify hepatocyte lipogenesis, to prime cytoprotective mechanisms, and reduce liver fibrogenesis.[52]

We report that fructose administration led to accumulation within the tissue and rapid transit into glycolytic and lipogenic pathways. DNL was facilitated by the generation of glycerol from fructose, and we also observed the conversion of pyruvate to alanine and lactate. Although accumulation of labelled fructose reflects direct uptake of labelled carbohydrate, fructose generation from glucose via the polyol pathway may be relevant over the timeframe of our experiments. This is supported by a reduction in labelled fructose in our inhibited samples (Fig. 4). Here aldose reductase would generate sorbitol from glucose and this could be modified by sorbitol dehydrogenase to fructose.[30] Excess concentrations of sorbitol are rapidly metabolised to fructose in an almost exclusively liver-dependent manner by this route.[53] We see an accumulation of label in sorbitol over time and also note that this was more pronounced in the presence of KHK inhibition. Notably the pattern was slightly different in the NASH context (Fig. S6) with quicker accumulation of labelled fructose and little change in labelled glucose over time. This may reflect the hyperactivity of the polyol pathway in NAFLD[54] and reduced reliance on fructose as a gluconeogenic precursor.

We noted a reduced hepatic activation of fructose-1 phosphate after KHK inhibition as expected[55] accompanied by a decrease in lactate, alanine, and glycerol that was particularly marked in cirrhotic livers. Elevated alanine and lactate after fructose exposure fit with NMR spectroscopy studies in patients with NAFLD. Here hepatic alanine and lactate concentrations, particularly when combined with TG concentrations showed promise as a tool to discriminate between simple steatosis and NASH.[56] Importantly, we observed no associated hepatocellular toxicity in our treated samples, genetically deficient mice exhibit normal lifespan and physiology, and early stage human trials in patients with NAFLD suggest the compound is well tolerated with no serious adverse events reported. Patients with hereditary fructosuria owing to KHK gene variants exhibit limited consequences unless fructose excess is ingested, whereupon there is a persistent rise in blood fructose levels and excretion of fructose into urine. This suggests that chronic administration of an inhibitor would not exhibit a mechanism-based safety issue.[14]

Thus, in conclusion, we have for the first time carried out NMR-based metabolic analysis of human liver which explains the hepatic consequences of fructose administration, and provide both human and murine evidence to support the benefit of using KHK inhibition to improve steatosis, fibrosis, and inflammation in patients with NAFLD.

Abbreviations

ALD, alcohol-related cirrhosis; aLMF, activated liver myofibroblasts; ALT, alanine transaminase; APRI, AST to Platelet Ratio Index; AST, aspartate transaminase; BEC, biliary epithelial cells; BSA, bovine serum albumin; CT, computed tomography; DNL, *de novo* lipogenesis; FIB4, fibrosis-4; G/F, glucose/fructose; HSCs, hepatic stellate cells; HSECs, hepatic sinusoidal endothelial cells; HSQC, heteronuclear single quantum coherence; IGF, insulin-like growth factor; KHK, ketohexokinase; KO, knockout; LGLI, low glucose and insulin; NAFLD, non-alcoholic fatty liver disease; NASH, non-alcoholic steatohepatitis; NPCs, non-parenchymal cells; PBC, primary biliary cholangitis; PDGF, platelet-derived growth factor; PSC, primary sclerosing cholangitis; TG, triglyceride; TGFB, transforming growth factor beta; TIMP-1, Tissue Inhibitor of Matrix metalloproteinase-1; WT, wild-type.

Financial support

This study includes independent research supported by the Birmingham National Institute for Health Research (NIHR) Birmingham Biomedical Research Centre, based at the University of Birmingham. The views expressed are those of the authors and not necessarily those of the NHS, the National Institute of Health Research or the Department of Health and Social Care. The work was part funded by a collaborative research grant to the University of Birmingham from Takeda Pharmaceuticals Inc. Both parties were involved in experimental design/data generation, and manuscript drafting.

Conflicts of interest

ELS, RS, EN, ULG, GH, and PFL have no conflicts of interest to declare. REF, BKC, SAH, MJL, MO, RAF, JER, and BRW are employees and stock holders of HemoShear Therapeutics. KM, HO, HY, JP, REF, NN, and DME are employees and stock holders of Takeda.

Please refer to the accompanying ICMJE disclosure forms for further details.

Authors' contributions

Study design and interpretation: ELS, RS, ULG, GH, PFL, HY, REF, BKC, RAF, JER, BRW, JP, DME.

Experimental data generation and analysis: ELS, RS, EN, KM, HO, HY, SAH, MJL, MO, RAF, NN, BRW.

Drafting manuscript ELS, RS, BKC, HY, GH, DME and PFL.

Approved the final version of the manuscript: all authors.

Data availability statement

Where possible, experimental data can be shared via contact with the corresponding author. This excludes commercially sensitive information or data relating to individual human tissue donors.

Supplementary data

Supplementary data to this article can be found online at https://doi.org/10.1016/j.jhepr.2020.100217.

References

[1] Than NN, Newsome PN. A concise review of non-alcoholic fatty liver disease. Atherosclerosis 2015;239:192–202.
[2] Chiu S, Sievenpiper JL, de Souza RJ, Cozma AI, Mirrahimi A, Carleton AJ, et al. Effect of fructose on markers of non-alcoholic fatty liver disease (NAFLD): a systematic review and meta-analysis of controlled feeding trials. Eur J Clin Nutr 2014;68:416–423.
[3] Wu S, Wu F, Ding Y, Hou J, Bi J, Zhang Z. Association of non-alcoholic fatty liver disease with major adverse cardiovascular events: A systematic review and meta-analysis. Sci Rep 2016;6:33386.
[4] Le KA, Ith M, Kreis R, Faeh D, Bortolotti M, Tran C, et al. Fructose overconsumption causes dyslipidemia and ectopic lipid deposition in healthy subjects with and without a family history of type 2 diabetes. Am J Clin Nutr 2009;89:1760–1765.
[5] Bray GA, Nielsen SJ, Popkin BM. Consumption of high-fructose corn syrup in beverages may play a role in the epidemic of obesity. Am J Clin Nutr 2004;79:537–543.
[6] Douard V, Ferraris RP. The role of fructose transporters in diseases linked to excessive fructose intake. J Physiol 2013;591:401–414.
[7] Vos MB, Kimmons JE, Gillespie C, Welsh J, Blanck HM. Dietary fructose consumption among US children and adults: the Third National Health and Nutrition Examination survey. Medscape J Med 2008;10:160.

[8] Lyssiotis CA, Cantley LC. Metabolic syndrome: F stands for fructose and fat. Nature 2013;502:181–182.
[9] Ouyang X, Cirillo P, Sautin Y, McCall S, Bruchette JL, Diehl AM, et al. Fructose consumption as a risk factor for non-alcoholic fatty liver disease. J Hepatol 2008;48:993–999.
[10] Softic S, Gupta MK, Wang GX, Fujisaka S, O'Neill BT, Rao TN, et al. Divergent effects of glucose and fructose on hepatic lipogenesis and insulin signaling. J Clin Invest 2017;127:4059–4074.
[11] Jegatheesan P, Beutheu S, Ventura G, Nubret E, Sarfati G, Bergheim I, et al. Citrulline and nonessential amino acids prevent fructose-induced nonalcoholic fatty liver disease in rats. J Nutr 2015;145:2273–2279.
[12] Allen RJ, Musante CJ. A mathematical analysis of adaptations to the metabolic fate of fructose in essential fructosuria subjects. Am J Physiol Endocrinol Metab 2018.
[13] Ishimoto T, Lanaspa MA, Le MT, Garcia GE, Diggle CP, Maclean PS, et al. Opposing effects of fructokinase C and A isoforms on fructose-induced metabolic syndrome in mice. Proc Natl Acad Sci U S A 2012;109:4320–4325.
[14] Maryanoff BE, O'Neill JC, McComsey DF, Yabut SC, Luci DK, Jordan AD Jr, et al. Inhibitors of Ketohexokinase: discovery of Pyrimidinopyrimidines with specific substitution that complements the ATP-binding site. ACS Med Chem Lett 2011;2:538–543.
[15] Bhogal RH, Afford SC. Factors affecting hepatocyte isolation, engraftment, and replication in an in vivo model. Liver Transpl 2010;16:1444. author reply 1445.
[16] Weston CJ, Shepherd EL, Claridge LC, Rantakari P, Curbishley SM, Tomlinson JW, et al. Vascular adhesion protein-1 promotes liver inflammation and drives hepatic fibrosis. J Clin Invest 2015;125:501–520.
[17] Heydtmann M, Lalor PF, Eksteen JA, Hubscher SG, Briskin M, Adams DH. CXC chemokine ligand 16 promotes integrin-mediated adhesion of liver-infiltrating lymphocytes to cholangiocytes and hepatocytes within the inflamed human liver. J Immunol 2005;174:1055–1062.
[18] Cole BK, Feaver RE, Wamhoff BR, Dash A. Non-alcoholic fatty liver disease (NAFLD) models in drug discovery. Expert Opin Drug Discov 2018;13:193–205.
[19] Feaver RE, Cole BK, Lawson MJ, Hoang SA, Marukian S, Blackman BR, et al. Development of an in vitro human liver system for interrogating nonalcoholic steatohepatitis. JCI Insight 2016;1:e90954.
[20] Trevaskis JL, Griffin PS, Wittmer C, Neuschwander-Tetri BA, Brunt EM, Dolman CS, et al. Glucagon-like peptide-1 receptor agonism improves metabolic, biochemical, and histopathological indices of nonalcoholic steatohepatitis in mice. Am J Physiol Gastrointest Liver Physiol 2012;302:G762–G772.
[21] Boland ML, Oro D, Tolbol KS, Thrane ST, Nielsen JC, Cohen TS, et al. Towards a standard diet-induced and biopsy-confirmed mouse model of non-alcoholic steatohepatitis: Impact of dietary fat source. World J Gastroenterol 2019;25:4904–4920.
[22] Saborano R, Eraslan Z, Roberts J, Khanim FL, Lalor PF, Reed MAC, et al. A framework for tracer-based metabolism in mammalian cells by NMR. Sci Rep 2019;9:2520.
[23] Delaglio F, Grzesiek S, Vuister GW, Zhu G, Pfeifer J, Bax A. NMRPipe: a multidimensional spectral processing system based on UNIX pipes. J Biomol NMR 1995;6:277–293.
[24] Hyberts SG, Milbradt AG, Wagner AB, Arthanari H, Wagner G. Application of iterative soft thresholding for fast reconstruction of NMR data non-uniformly sampled with multidimensional Poisson Gap scheduling. J Biomol NMR 2012;52:315–327.
[25] Ludwig C, Gunther UL. MetaboLab–advanced NMR data processing and analysis for metabolomics. BMC Bioinform 2011;12:366.
[26] Clapper JR, Hendricks MD, Gu G, Wittmer C, Dolman CS, Herich J, et al. Diet-induced mouse model of fatty liver disease and nonalcoholic steatohepatitis reflecting clinical disease progression and methods of assessment. Am J Physiol Gastrointest Liver Physiol 2013;305:G483–G495.
[27] Ramachandran P, Dobie R, Wilson-Kanamori JR, Dora EF, Henderson BEP, Luu NT, et al. Resolving the fibrotic niche of human liver cirrhosis at single-cell level. Nature 2019;575:512–518.
[28] Stanhope KL, Schwarz JM, Keim NL, Griffen SC, Bremer AA, Graham JL, et al. Consuming fructose-sweetened, not glucose-sweetened, beverages increases visceral adiposity and lipids and decreases insulin sensitivity in overweight/obese humans. J Clin Invest 2009;119:1322–1334.
[29] Stanhope KL, Havel PJ. Fructose consumption: recent results and their potential implications. Ann N Y Acad Sci 2010;1190:15–24.
[30] Lanaspa MA, Ishimoto T, Li N, Cicerchi C, Orlicky DJ, Ruzycki P, et al. Endogenous fructose production and metabolism in the liver contributes to the development of metabolic syndrome. Nat Commun 2013;4:2434.
[31] Jegatheesan P, Beutheu S, Ventura G, Sarfati G, Nubret E, Kapel N, et al. Effect of specific amino acids on hepatic lipid metabolism in fructose-induced non-alcoholic fatty liver disease. Clin Nutr 2016;35:175–182.
[32] Pinnick KE, Hodson L. Challenging metabolic tissues with fructose: tissue-specific and sex-specific responses. J Physiol 2019;597:3527–3537.
[33] Tobin V, Le Gall M, Fioramonti X, Stolarczyk E, Blazquez AG, Klein C, et al. Insulin internalizes GLUT2 in the enterocytes of healthy but not insulin-resistant mice. Diabetes 2008;57:555–562.
[34] Douard V, Ferraris RP. Regulation of the fructose transporter GLUT5 in health and disease. Am J Physiol Endocrinol Metab 2008;295:E227–E237.
[35] Legeza B, Balazs Z, Odermatt A. Fructose promotes the differentiation of 3T3-L1 adipocytes and accelerates lipid metabolism. FEBS Lett 2014;588:490–496.
[36] Shu R, David ES, Ferraris RP. Luminal fructose modulates fructose transport and GLUT-5 expression in small intestine of weaning rats. Am J Physiol 1998;274:G232–G239.
[37] Cox CL, Stanhope KL, Schwarz JM, Graham JL, Hatcher B, Griffen SC, et al. Consumption of fructose- but not glucose-sweetened beverages for 10 weeks increases circulating concentrations of uric acid, retinol binding protein-4, and gamma-glutamyl transferase activity in overweight/obese humans. Nutr Metab (Lond) 2012;9:68.
[38] Williamson RM, Price JF, Glancy S, Perry E, Nee LD, Hayes PC, et al. Prevalence of and risk factors for hepatic steatosis and nonalcoholic Fatty liver disease in people with type 2 diabetes: the Edinburgh Type 2 Diabetes study. Diabetes Care 2011;34:1139–1144.
[39] Andres-Hernando A, Li N, Cicerchi C, Inaba S, Chen W, Roncal-Jimenez C, et al. Protective role of fructokinase blockade in the pathogenesis of acute kidney injury in mice. Nat Commun 2017;8:14181.
[40] Lanaspa MA, Sanchez-Lozada LG, Cicerchi C, Li N, Roncal-Jimenez CA, Ishimoto T, et al. Uric acid stimulates fructokinase and accelerates fructose metabolism in the development of fatty liver. PLoS One 2012;7:e47948.
[41] Jegatheesan P, De Bandt JP. Hepatic steatosis: a role for citrulline. Curr Opin Clin Nutr Metab Care 2016.
[42] Bergheim I, Weber S, Vos M, Kramer S, Volynets V, Kaserouni S, et al. Antibiotics protect against fructose-induced hepatic lipid accumulation in mice: role of endotoxin. J Hepatol 2008;48:983–992.
[43] Lanaspa MA, Sanchez-Lozada LG, Choi YJ, Cicerchi C, Kanbay M, Roncal-Jimenez CA, et al. Uric acid induces hepatic steatosis by generation of mitochondrial oxidative stress: potential role in fructose-dependent and -independent fatty liver. J Biol Chem 2012;287:40732–40744.
[44] Smith JA, Stallons LJ, Schnellmann RG. Renal cortical hexokinase and pentose phosphate pathway activation through the EGFR/Akt signaling pathway in endotoxin-induced acute kidney injury. Am J Physiol Ren Physiol 2014;307:F435–F444.
[45] Jang C, Hui S, Lu W, Cowan AJ, Morscher RJ, Lee G, et al. The small intestine converts dietary fructose into glucose and organic acids. Cell Metab 2018;27:351–361 e353.
[46] Prigge JR, Coppo L, Martin SS, Ogata F, Miller CG, Bruschwein MD, et al. Hepatocyte Hyperproliferation upon Liver-Specific Co-disruption of Thioredoxin-1, Thioredoxin Reductase-1, and Glutathione Reductase. Cell Rep 2017;19:2771–2781.
[47] Yeligar SM, Machida K, Kalra VK. Ethanol-induced HO-1 and NQO1 are differentially regulated by HIF-1alpha and Nrf2 to attenuate inflammatory cytokine expression. J Biol Chem 2010;285:35359–35373.
[48] Cox CL, Stanhope KL, Schwarz JM, Graham JL, Hatcher B, Griffen SC, et al. Circulating concentrations of monocyte chemoattractant protein-1, plasminogen activator inhibitor-1, and soluble leukocyte adhesion molecule-1 in overweight/obese men and women consuming fructose- or glucose-sweetened beverages for 10 weeks. J Clin Endocrinol Metab 2011;96:E2034–E2038.
[49] Cirillo P, Gersch MS, Mu W, Scherer PM, Kim KM, Gesualdo L, et al. Ketohexokinase-dependent metabolism of fructose induces proinflammatory mediators in proximal tubular cells. Journal of the American Society of Nephrology : JASN 2009;20:545–553.
[50] Bonacchi A, Romagnani P, Romanelli RG, Efsen E, Annunziato F, Lasagni L, et al. Signal transduction by the chemokine receptor CXCR3: activation of Ras/ERK, Src, and phosphatidylinositol 3-kinase/Akt controls cell migration and proliferation in human vascular pericytes. JBiolChem 2001;276:9945–9954.
[51] de Mesquita FC, Bitencourt S, Caberlon E, da Silva GV, Basso BS, Schmid J, et al. Fructose-1,6-bisphosphate induces phenotypic reversion of activated hepatic stellate cell. Eur J Pharmacol 2013;720:320–325.
[52] Lanaspa MA, Andres-Hernando A, Orlicky DJ, Cicerchi C, Jang C, Li N, et al. Ketohexokinase C blockade ameliorates fructose-induced metabolic dysfunction in fructose-sensitive mice. J Clin Invest 2018;128:2226–2238.

[53] van der Hoven B, van Pelt H, Swart EL, Bonthuis F, Tilanus HW, Bakker J, et al. Noninvasive functional liver blood flow measurement: comparison between bolus dose and steady-state clearance of sorbitol in a small-rodent model. Am J Physiol Gastrointest Liver Physiol 2010;298:G177–G181.
[54] Hotta N, Kawamura T, Umemura T. Are the polyol pathway and hyperuricemia partners in the development of non-alcoholic fatty liver disease in diabetes? J Diabetes Investig 2019.
[55] Geidl-Flueck B, Gerber PA. Insights into the hexose liver metabolism-glucose versus fructose. Nutrients 2017;9.
[56] Kim TH, Jun HY, Kim KJ, Lee YH, Lee MS, Choi KH, et al. Hepatic alanine differentiates nonalcoholic steatohepatitis from simple steatosis in humans and mice: A proton MR spectroscopy study with long echo time. J Magn Reson Imaging 2017;46:1298–1310.